Electronic Supplementary Material (ESI) for Journal of Materials Chemistry C.

Fig. S1. Photographs, XRD patterns, and SEM images of the Ni electrode and PMNZT ceramic annealed at various temperatures (200–500 °C). (a) Photographs of Ni-printed PMNZT. (b) XRD patterns of PMNZT (left), and NiO and Ni (right). (c) XRD patterns of PMNZT at different annealing temperatures. (d) Lattice parameters and c/a ratio of PMNZT.

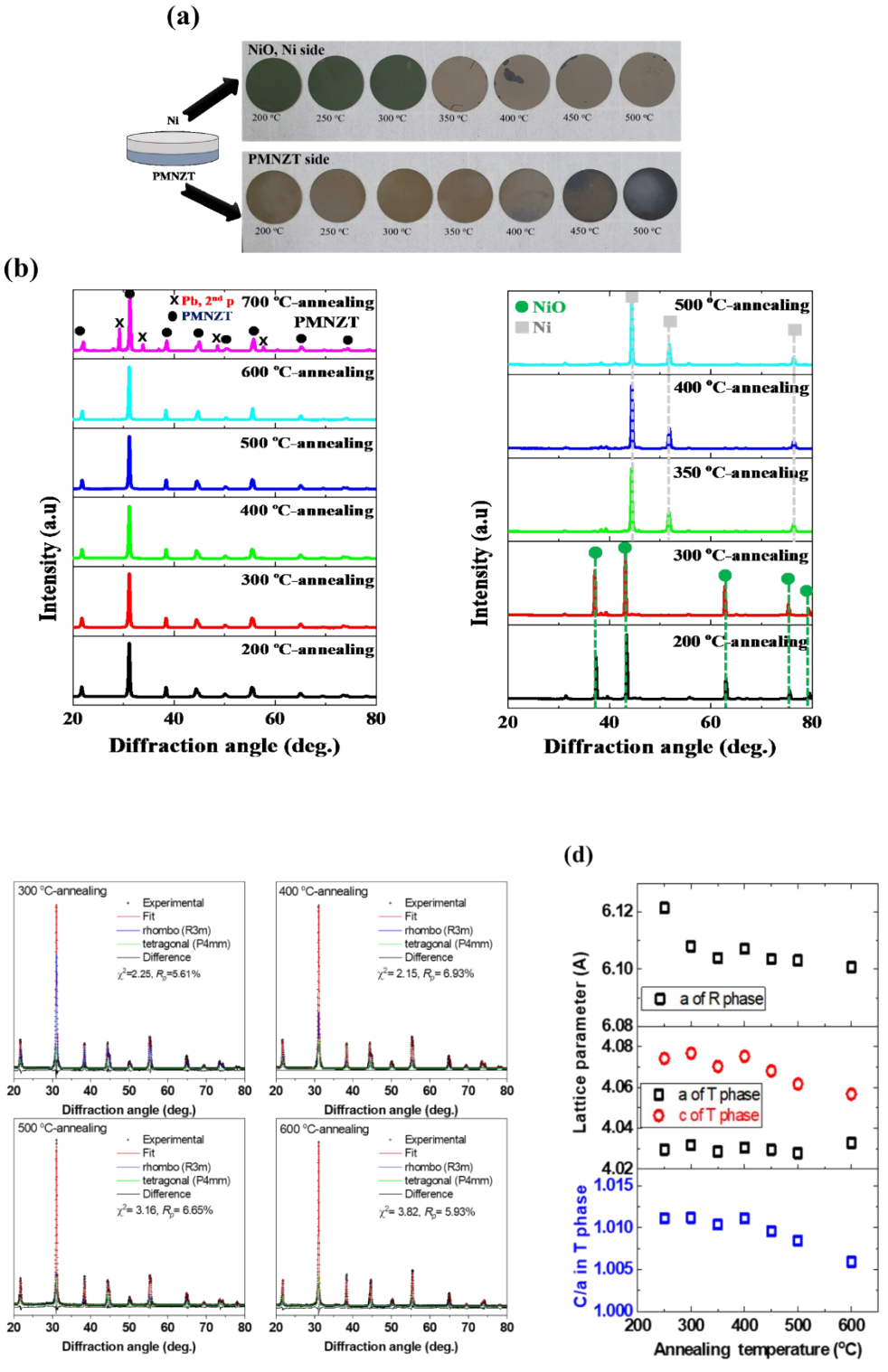

Fig. S2 Polarization–electric-field curves of PMNZT before and after annealing at 400, 500, or 600 °C. PMNZT was fabricated by the conventional powder-compaction and sintering methods.

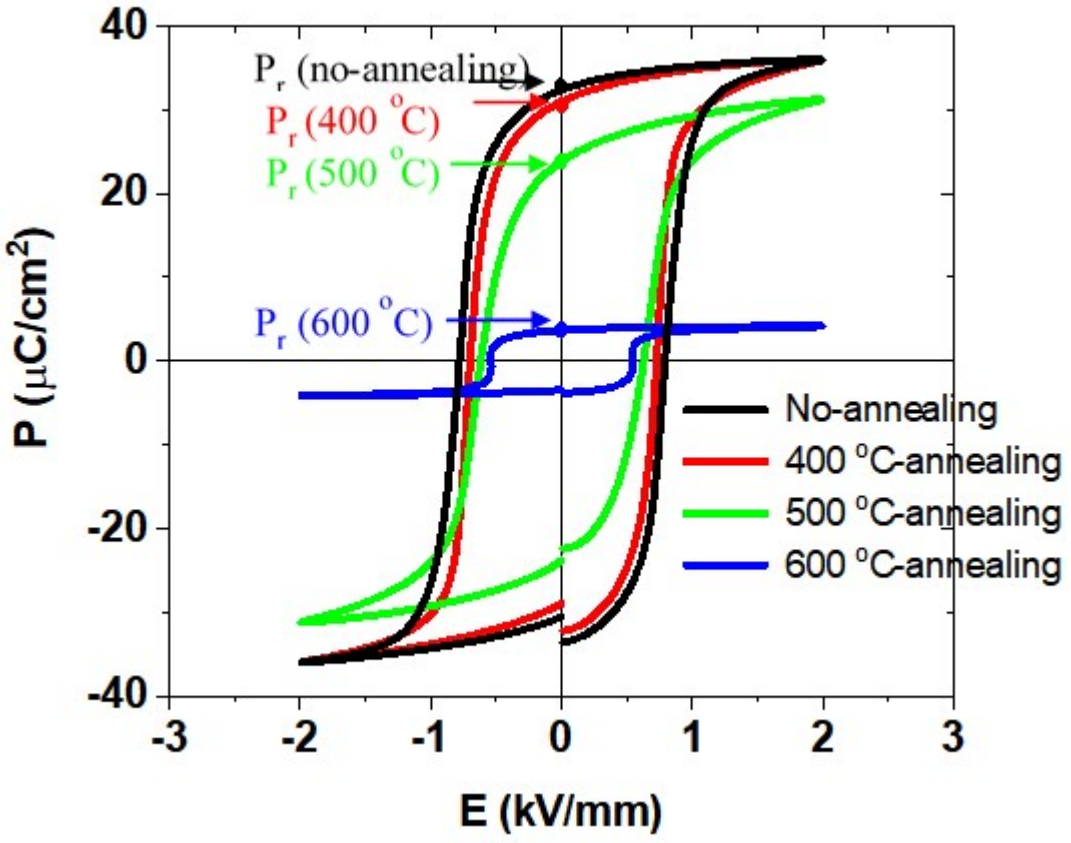

Samples were fabricated by printing Ni paste onto one side of a PMNZT sheet, followed by sintering at 1150 °C in air and annealing at temperatures ranging from 200 to 700 °C under N_2–H_2 gas flow. Photographs of the Ni-printed PMNZT bulks samples were acquired after annealing (Fig. 3a). The electrode of the samples annealed at 200–300 °C had a green color, indicating the presence of NiO. The electrode was silvery white after annealing at 350 °C, which is characteristic of metallic Ni. Further, the typical yellow–white color of a piezoelectric ceramic was observed on the PMNZT side after annealing at temperatures up to 400 °C. The ceramic side became dark after annealing at 500 °C. However, the phase of the ceramic was still stable, as confirmed by X-ray diffraction (XRD) analysis of samples annealed at 350 to 500 °C (**Supplementary Data Fig**. **S1**). In general, NiO and PMNZT

were not reactive during annealing below 300 °C, while NiO was converted to metallic Ni between 350 and 500 °C. However, annealing at 700 °C and above led to the decomposition of PMNZT to PbO. Consequently, the conversion to Ni and simultaneous stability of PMNZT were ensured during annealing between 350 and 500 °C. Although XRD analysis indicated that PMNZT was stable, the stability of the crystal structure remains questionable, and the formation of point defects (e.g., oxygen and cation vacancies) may have occurred.

Further analysis of the XRD patterns, including the Rietveld refinements, was conducted. The lattice constant and dielectric properties of the reduced PMNZT were investigated to identify any changes in the PMNZT after annealing at the various temperatures (**Supplementary Data Fig**. **S1**). The lattice constants (*a* and *c*) were determined, and the *c*/*a* ratios of the tetragonal (P4mm) and rhombohedral (R3m) phases changed by ~0.02% due to an increase in *a* and decrease in *c* after annealing. A similar change in remnant polarization (P_r) was also noted after annealing (**Supplementary Data Fig. S2**), where annealing at temperatures above 500 °C led to a change in the polarization curve and a decrease in P_r. These findings clearly demonstrate that annealing led to a slight modification of PMNZT.

The formation of Pb or oxygen defects in PMNZT is expected under exposure to reducing conditions [45, 46]. The electrode material and the perovskite oxide ceramic were expected to have differences in stability under the reducing conditions of N_2–H_2 gas flow, where significant decomposition of NiO occurred while the PMNZT perovskite did not react. A previous study reported that oxygen atoms in the ABO_3 structure were strongly bonded to a B-site cation in the BO_6 octahedron [16]. The phase stability difference between PMNZT and NiO was similar to the bonding characteristics of the cation and oxygen in the ABO_3 and MO structures. The Ni–O bonds were weaker than the Ti–O bonds in PZT, thus NiO was less resistant to reduction when exposed to the H_2 atmosphere. The microstructure of the annealed Ni comprised a dense NiO grain structure when annealed at ~200 to 300 °C, while porous grains were observed after annealing at 350 °C and higher (Fig. 3a). The pore size increased with increasing annealing temperature due to the formation of gas and removal of oxygen from the electrode during reduction, giving rise to the isolated void patterns observed in the sample

annealed at 350 °C. As the annealing temperature was increased to 500 °C, larger pores were formed and recrystallization occurred, leading to the growth of Ni grains. The equiaxed pores had diameter of 100–500 nm, and no residual NiO was observed behind the reaction front [41]. Further, annealing at 500 and 600 °C led to the formation of dense Ni grains and collapsed pores due to Ni recrystallization.

Fig. S3 Raman spectra and transmission electron microscopy (TEM) images of Ni–PMNZT devices. (a) Raman spectra of Ni-PMNZT (top), NiO-PMNZT (middle), and pure PMNZT (bottom). (b) EPMA illustrating the elemental distribution in the Ni–PMNZT devices.

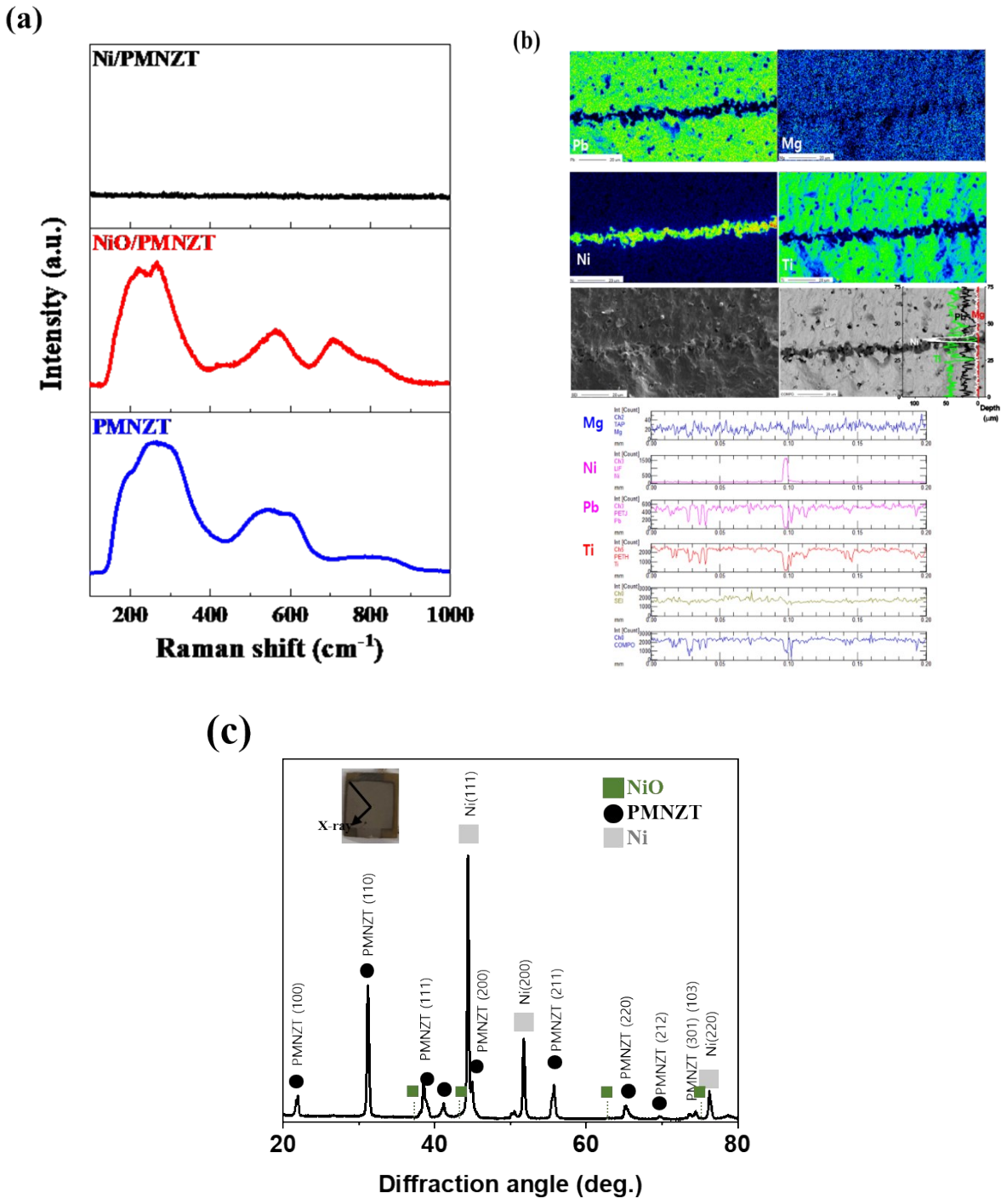

The interfacial stability between Ni and PMNZT was evaluated based on Raman spectroscopy and TEM. Raman spectroscopy is a spectroscopic technique used to observe vibrational, rotational, and other low-frequency modes in a system, and provided an insight into the transition of the NiO to porous Ni in the Ni–PMNZT sample. The Raman spectra of PZT, NiO, and Ni were used to further evaluate the local ionic configuration of NiO and Ni (Fig. 5) [45-46]. The NiO spectrum had five characteristic NiO phonon modes located at 180, 260, 300, 514 and 712 cm^{-1}. An increase in the vibrational amplitude indicates a change in the local crystal structure. The decrease in the Raman intensity for NiO was accompanied by an increase in the spectral response for metal Ni, while PMNZT remained stable. None of the five characteristic peaks of NiO were observed in the spectrum of the completely reduced Ni sample due to the disappearance of polarization associated with Ni–O ionic bonding (Supplementary Data Fig. S3).

The macrostructure of the Ni-PMNZT device was analyzed using scanning electron microscopy (SEM) and electron probe microanalysis (EPMA) (Supplementary Data Fig. S3). Elemental Ni was detected in the electrode, but no diffusion of Ni was detected in the EPMA line profiles.